

1 **Speciation in the face of gene flow within the toothed whale superfamily Delphinoidea**

2
3 Michael V Westbury^{1*}, Andrea A. Cabrera¹, Alba Rey-Iglesia¹, Binia De Cahsan¹, Stefanie
4 Hartmann², Eline D Lorenzen^{1*}

5 1. The GLOBE Institute, University of Copenhagen, Øster Voldgade 5-7, Copenhagen,
6 Denmark

7 2. Institute of Biochemistry and Biology, University of Potsdam, Karl-Liebknecht-Str.
8 24-25, Potsdam, Germany

9
10 * Corresponding authors: m.westbury@sund.ku.dk, eline.lorenzen@sund.ku.dk

11 **Abstract**

12
13
14 Understanding speciation is a central aspect in Biology. The formation of new species
15 was once thought to be a simple bifurcation process. However, recent advances in genomic
16 resources now provide the opportunity to investigate the role of post-divergence gene flow in
17 the speciation process. The diversification of lineages in the presence of gene flow appears
18 almost paradoxical. However, with enough time and in the presence of incomplete physical
19 and/or ecological barriers to gene flow, speciation can and does occur. Speciation without
20 complete isolation seems especially likely to occur in highly mobile, wide ranging marine
21 species, such as cetaceans, which face limited geographic barriers. The toothed whale
22 superfamily Delphinoidea represents a good example to further explore speciation in the
23 presence of interspecific gene flow. Delphinoidea consists of three families (Delphinidae,
24 Phocoenidae, and Monodontidae) and within all three families, contemporary interspecific
25 hybrids have been reported. Here, we utilise publicly available genomes from nine species,
26 representing all three families, to investigate signs of post-divergence gene flow across their
27 genomes, and to address the speciation processes that led to the diversity seen today within
28 Delphinoidea. We use a multifaceted approach including: (i) phylogenetics, (ii) the
29 distribution of shared derived alleles, and (iii) demography-based. We find that the
30 divergence and evolution of lineages in Delphinoidea did not follow a simple bifurcating
31 pattern, but were much more complex. Our results indicate multiple, long-lasting ancestral
32 gene flow events both within and among families, which continued for millions of years after
33 initial divergence.

34 **Introduction**

35
36
37 The formation of new species involves the divergence of lineages through
38 reproductive isolation. Such isolation can initially occur in allopatry (geographical isolation)
39 or in sympatry (biological/ecological isolation). Over time, these barriers are maintained and
40 strengthened, ultimately leading to the formation of new species (Norris and Hull, 2012).
41 While allopatric speciation requires geographical isolation plus time, sympatric speciation
42 often requires a broader and more complicated set of mechanisms (Turelli et al., 2001). These
43 mechanisms mostly rely on ecologically-mediated natural selection. Parapatric speciation, on

44 the other hand, encompasses intermediate scenarios of partial, but incomplete, physical
45 restrictions to gene flow leading to speciation.

46

47 Through the analysis of whole-genome datasets, the detection of post-divergence gene
48 flow between distinct species is becoming more commonplace (Árnason et al., 2018; Barlow
49 et al., 2018; Westbury et al., 2020), demonstrating that speciation is much more complex than
50 a simple bifurcating process (Campbell and Poelstra, 2018; Feder et al., 2012). Speciation is
51 not an instantaneous process, but requires tens of thousands to millions of generations to
52 achieve complete reproductive isolation (Butlin and Smadja, 2018; Coyne and Orr, 2004; Liu
53 et al., 2014). The duration it takes to reach this isolation may be especially long in highly
54 mobile marine species, such as cetaceans, due to a relative lack of geographic barriers in the
55 marine realm, and therefore high potential for gene flow (Árnason et al., 2018).

56

57 The apparent inability to undergo allopatric speciation in marine species has been
58 termed the marine-speciation paradox (Bierne et al., 2003). However, over the past decade,
59 genomic studies have provided some insights into how speciation can occur within cetaceans
60 (Árnason et al., 2018; Moura et al., 2020). For example, in killer whales (*Orcinus orca*) it has
61 been proposed that initial phases of allopatry may have led to the accumulation of ecological
62 differences between populations, which strengthened population differences even after they
63 came into secondary contact (Foote et al., 2011; Foote and Morin, 2015). However, whether
64 these initial phases of allopatry caused the divergence, or whether speciation occurred purely
65 in sympatry, remains debated (Moura et al., 2015). Yet these two hypotheses are not
66 necessarily mutually exclusive. Instead, differentiation in parapatry, encompassing features of
67 both allopatric and sympatric speciation, may have been key in the evolutionary history of
68 cetaceans.

69

70 The toothed whale superfamily Delphinoidea represents an interesting opportunity to
71 further explore speciation in the presence of putative interspecific gene flow. The root of
72 Delphinoidea has been dated to ~19 million years ago (Ma) (95% CI 19.73 - 18.26 Ma)
73 (McGowen et al., 2020) and has given rise to three families: (i) Delphinidae, the most species
74 rich family, which comprises dolphins and ‘black-fish’ (such as killer whales and pilot
75 whales (*Globicephala spp.*)); (ii) Phocoenidae, commonly known as porpoises; and (iii)
76 Monodontidae, which comprises two surviving lineages, belugas (*Delphinapterus leucas*) and
77 narwhals (*Monodon monoceros*).

78

79 Delphinoidea is of particular interest, as contemporary interspecific hybrids have been
80 reported within all three families: Delphinidae (Espada et al., 2019; Miyazaki et al., 1992;
81 Silva et al., 2005), Phocoenidae (Willis et al., 2004), and Monodontidae (Skovrind et al.,
82 2019). However, these hybrids represent recent hybridization events that occurred long after
83 species divergence, and their contributions to the parental gene pools is mostly unknown. The
84 presence of more ancient introgressive hybridization events between families, and during the
85 early radiations of these families, has yet to be investigated. With the rapid increase of
86 genomic resources for cetaceans, and in particular for species within Delphinoidea, we are

87 presented with the ideal opportunity to investigate post-divergence gene flow between
88 lineages, furthering our understanding of speciation processes in cetaceans.

89

90 Here, we utilise publicly available whole-genome data from nine species of
91 Delphinoidea, representing all three families, to investigate signs of post-divergence gene
92 flow across their genomes. Our analyses included five Delphinidae (killer whale, Pacific
93 white-sided dolphin (*Lagenorhynchus obliquidens*), long-finned pilot whale (*Globicephala*
94 *melas*), bottlenose dolphin (*Tursiops truncatus*), Indo-Pacific bottlenose dolphin (*T.*
95 *aduncus*)); two Phocoenidae (harbour porpoise (*Phocoena phocoena*), finless porpoise
96 (*Neophocaena phocaenoides*)); and two Monodontidae (beluga, narwhal). Moreover, we
97 compare their species-specific genetic diversity and demographic histories, and explore how
98 species abundances may have played a role in interspecific hybridisation over the last two
99 million years.

100

101 **Results and discussion**

102

103 **Detecting gene flow**

104 To assess the evolutionary relationships across the genomes of the nine Delphinoidea
105 species investigated, we computed non-overlapping sliding-window maximum-likelihood
106 phylogenies of four different window sizes in RAxML (Stamatakis, 2014). These analyses
107 resulted in 43,207 trees (50 kilobase (kb) windows), 21,387 trees (100 kb windows), 3,705
108 trees (500 kb windows), and 1,541 trees (1 megabase (Mb) windows) (Fig. 1, Supplementary
109 Fig. S1). Regardless of window size, we retrieve consensus support for the species tree
110 previously reported using target sequence capture (McGowen et al., 2020). However, when
111 considering the smallest window size (50 kb), we find a considerable proportion of trees (up
112 to 76%) with an alternative topology to the known species tree (Fig. 1A). These alternative
113 topologies could be due to incomplete lineage sorting (ILS) or interspecific gene flow
114 (Leaché et al., 2014). Moreover, the higher prevalence of this pattern in the 50 kb windows
115 (21% of windows show an alternative topology in the 1 Mb dataset (Fig. 1B)), may indicate
116 that inconsistencies in topology are caused by ancient, rather than recent, events.

117

118 To further explore potential gene flow while taking ILS into account, we applied D-
119 statistics. D-statistics uses a four-taxon approach [[[H1, H2], H3], Outgroup] to uncover the
120 differential distribution of shared derived alleles, which may represent gene flow between
121 either H1/H3 or H2/H3. Here we used baiji (*Lipotes vexillifer*) as the outgroup, and alternated
122 the ingroup positions based on the consensus topology. We find that 85 out of 86 tests show
123 signs of gene flow within and between families (Supplementary table S1), suggesting the
124 evolutionary history of Delphinoidea is very complex.

125

126 Due to the inability of the four-taxon D-statistics approach to detect the direction of
127 gene flow, as well as whether gene flow events may have occurred between ancestral
128 lineages, we used D-foil. D-foil enables further characterization of the D-statistics results,
129 which may be particularly relevant, given the complex array of gene flow putatively present
130 within Delphinoidea. D-foil uses a five-taxon approach [[H1, H2] [H3, H4], Outgroup] and a

131 system of four independent D-statistics in a sliding-window fashion to uncover (i) putative
132 gene flow events, (ii) donor and recipient lineages, and (iii) whether gene flow events
133 occurred between a distantly related lineage and the ancestor of two sister lineages, which is
134 indicative of ancestral lineage gene flow. However, due to the input topology requirements of
135 D-foil, we were only able to investigate gene flow between families, and not within families,
136 using this analysis. Hence, we tested for gene flow between Delphinidae/Phocoenidae,
137 Delphinidae/Monodontidae, and Monodontidae/Phocoenidae.

138

139 The D-foil results underscore the complex pattern of post-divergence gene flow
140 between families indicated by the D-statistics. We find support for interfamilial gene flow
141 events between all nine species investigated, to varying extents (Supplementary table S2).
142 This could reflect multiple episodes of gene flow between all investigated species.
143 Alternatively, the pattern could reflect ancient gene flow events between the ancestors of H1-
144 H2 and H3-H4 (in the topology [[H1, H2] [H3, H4], Outgroup]), with differential inheritance
145 of the admixed loci in subsequent lineages. Such ancestral gene flow events have previously
146 been shown to lead to false positives between species pairs using D-statistics (Moodley et al.,
147 2020). A further putative problem with these results can be seen when implementing D-foil
148 on the topology [[Delphinidae, Delphinidae], [Monodontidae, Phocoenidae], Outgroup]. We
149 find the majority of windows support a closer relationship between Delphinidae (ancestors of
150 H1 and H2) and Monodontidae (H3), as opposed to the species tree. If this result is correct, it
151 suggests the input topology was incorrect, implying that Delphinidae and Monodontidae are
152 sister lineages, as opposed to Phocoenidae and Monodontidae. However, this contrasts with
153 the family topology of [Delphinidae, [Phocoenidae, Monodontidae]] retrieved in our
154 phylogenetic analyses (Fig. 1) and reported by others (McGowen et al., 2020; Steeman et al.,
155 2009). Instead, we suggest our result reflects the limited ability of D-foil to infer gene flow
156 between these highly divergent lineages.

157

158 False positives and potential biases in D-statistics and D-foil can arise due to a
159 number of factors including (i) ancestral population structure, (ii) introgression from
160 unsampled and/or extinct ghost lineages, (iii) differences in relative population size of
161 lineages or in the timing of gene flow events, (iv) different evolutionary rates or sequencing
162 errors between H1 and H2, and (v) gene flow between ancestral lineages (Moodley et al.,
163 2020; Slatkin and Pollack, 2008; Zheng and Janke, 2018). These issues are important to
164 consider when interpreting our results, as the deep divergences of lineages suggest there were
165 probably a number of ancestral gene flow events, as well as gene flow events between now-
166 extinct lineages, that may bias results.

167

168 **Cessation of gene flow**

169 To further elucidate the complexity of interspecific gene flow within Delphinoidea,
170 we implemented F1 hybrid PSMC (hPSMC) (Cahill et al., 2016). This method creates a
171 pseudo-diploid sequence by merging pseudo-haploid sequences from two different genomes,
172 which in our case represents two different species. The variation in the interspecific pseudo-
173 F1 hybrid genome cannot coalesce more recently than the emergence of reproductive

174 isolation between the two parental species, and the method can therefore be used to infer
175 when gene flow between species ceased.

176

177 When considering the uppermost limit of when gene flow ended (equating to the most
178 ancient date) and the lower confidence interval of each divergence date (equating to the most
179 recent date), the majority of comparisons (29/36) show that gene flow continued for >50% of
180 the post-divergence branch length (Fig. 2, Supplementary results). This finding suggests that
181 reaching complete reproductive isolation in Delphinoidea was a slow process. Long-term,
182 continuous gene flow may reflect the ability of these cetacean species to travel long
183 distances, and the lack of significant geographical barriers in the marine environment.

184

185 Despite our finding of long-term, continued gene flow in the majority of comparisons,
186 our results suggest gene flow ceased more rapidly within Delphinidae, relative to within
187 Phocoenidae and Monodontidae (Fig. 2). Only three out of ten pairwise comparisons (killer
188 whale vs. Indo-Pacific white-sided dolphin, killer whale vs long-finned pilot whale, and
189 bottlenose dolphin vs Indo-Pacific bottlenose dolphin), showed continued gene flow for
190 >50% of the branch length post divergence. The remaining seven comparisons showed
191 continued gene flow along 48% - 24% of the post-divergence branch length. This finding
192 may reflect the inability of hPSMC to detect low levels of migration until the present day,
193 leading to large estimated intervals around the time point at which gene flow stopped.

194

195 Simulations have shown that in the presence of only 1/10,000 migrants per
196 generation, hPSMC suggests continued gene flow. However, this does not happen with a
197 lower rate of ~1/100,000 migrants per generation. Rather, in the latter case, the exponential
198 increase in N_e of the pseudo-hybrid genome, which is used to infer the date at which gene
199 flow ceased between the parental individuals, becomes a more gradual transition, leading to a
200 larger estimated time interval (Cahill et al., 2016). Within Delphinidae, we observe a
201 corresponding, less pronounced increase in N_e in the pseudo-hybrids, suggestive of
202 continued, but very low migration rates (Supplementary results). This finding suggests gene
203 flow within Delphinidae may have continued for longer than shown by hPSMC, which may
204 not be sensitive enough to detect the low rates of recent gene flow. Furthermore, persistent
205 gene flow is supported by confirmed fertile contemporary hybrids between some of our study
206 species; for example, bottlenose dolphins can produce fertile offspring with both Indo-Pacific
207 bottlenose dolphins (Gridley et al., 2018) and Pacific white-sided dolphins (Crossman et al.,
208 2016; Miyazaki et al., 1992). Either way, our hPSMC results within and between all three
209 families show a consistent pattern of long periods of interspecific migration in Delphinoidea,
210 some lasting up to more than ten million years post divergence.

211

212 **Interspecific hybridisation**

213 Interspecific hybridization may occur at a higher rate during periods of low
214 abundance, when a given species encounters only a limited number of conspecifics
215 (Crossman et al., 2016; Edwards et al., 2011; Westbury et al., 2019), and individuals may
216 mate with a closely related species instead of investing energy in finding a rarer conspecific
217 mate. To explore the relationship between susceptibility to interspecific hybridisation and

218 population size, we calculated the level of genome-wide genetic diversity for each species, as
219 a proxy for their population size (Fig. 3A). Narwhal, killer whale, beluga and long-finned
220 pilot whale have the lowest diversity levels, and should therefore be more susceptible to
221 interspecific hybridization events. A beluga/narwhal hybrid has been reported (Skovrind et
222 al., 2019), as has hybridisation between long-finned and short-finned pilot whales (Miralles et
223 al., 2016). However, hybrids between species with high genetic diversity, including harbour
224 porpoise (Willis et al., 2004), Indo-Pacific bottlenose dolphin (Baird et al., 2012), and
225 bottlenose dolphin (Espada et al., 2019; Herzingl and Johnsonz, 1997) have also been
226 reported, suggesting genetic diversity alone is not a good proxy for susceptibility to
227 hybridisation.

228

229 To investigate whether interspecific gene flow took place during past periods of low
230 population size, we estimated changes in intraspecific genetic diversity through time (Fig.
231 3B-D). The modeled demographic trajectories span the past two million years using a
232 Pairwise Sequentially Markovian Coalescent model (PSMC). We could therefore assess the
233 relationship for the three species pairs where the interval for the cessation of gene flow was
234 contained within this period: harbour/finless porpoise (Phocoenidae), beluga/narwhal
235 (Monodontidae), and bottlenose/Indo-pacific bottlenose dolphin (Delphinidae) (Fig. 2).

236

237 In the harbour porpoise, we observe an increase in effective population size (N_e)
238 beginning ~1 Ma, the rate of which increases further ~500 thousands of years ago (kya) (Fig.
239 3C). The timing of expansion overlaps the period during which gene flow with the finless
240 porpoise ceased (~1.1 - 0.5 Ma, Fig. 2), suggesting gene flow between the two species
241 occurred when population size in the harbour porpoise was lower. We observe a similar
242 pattern in belugas; an increase in N_e ~1 Ma, relatively soon after the proposed cessation of
243 gene flow with narwhals ~1.8 - 1.2 Ma (Fig. 3D). An increase in N_e may coincide with an
244 increase in relative abundance, which would increase the number of potential conspecific
245 mates, and in turn reduce the level of interspecific gene flow. Although we are unable to test
246 the direction and levels of gene flow between these species pairs, we expect a relative
247 reduction of gene flow into the more abundant species. A relative reduction of such events
248 would in turn lessen genomic signs of interspecific gene flow, despite its occurrence.

249

250 We observe a different pattern in the bottlenose/Indo-pacific bottlenose dolphins. In
251 the previous examples, we find relatively low population size when gene flow was ongoing,
252 and only in one of the two hybridizing species. In the dolphins, we find relatively high
253 population size during the period of gene flow in both species; N_e declines ~1 - 0.5 Ma,
254 coinciding with the putative end of gene flow ~1.2 - 0.4 Ma. The decline in N_e could either
255 reflect a decline in abundance, or a loss of connectivity between the two species. In the latter,
256 we expect levels of intraspecific diversity (and thereby inferred N_e) to decline with the
257 cessation of gene flow, even if absolute abundances did not change. This is indeed suggested
258 by our data, which shows both species undergoing the decline simultaneously, indicative of a
259 common cause.

260

261 Seven of the nine Delphinoidea genomes investigated show a similar pattern of a
262 rapid decline in N_e starting ~150 - 100 kya (Fig. 3B-D; the exceptions are narwhal and
263 Pacific white-sided dolphin). This concurrent decline could represent actual population
264 declines across species, or alternatively, simultaneous reductions in connectivity among
265 populations within each species. Based on similar PSMC analyses, a decline in N_e at this
266 time has also been reported in four baleen whale species (Árnason et al., 2018). Although this
267 could reflect demographic factors, such as the loss of population connectivity, the unique life
268 histories, distributions, and ecology of these cetacean species suggests that decreased
269 population connectivity is unlikely to have occurred simultaneously across all studied
270 species. Rather, the species-wide pattern may reflect climate-driven environmental change.

271
272 The period 150 - 100 kya overlaps with the onset of the last interglacial, when sea
273 levels increased to levels as high, if not higher, than at present (Polyak et al., 2018), and
274 which may have had a marine-wide effect on population sizes. A similar marine-wide effect
275 has been observed among baleen whales and their prey species in the Southern and North
276 Atlantic Oceans during the Pleistocene-Holocene climate transition (12-7 kya) (Cabrera et al.,
277 2018). These results lend support to the ability of marine-wide environmental shifts to drive
278 changes in population sizes across multiple species.

279
280 We suggest species-wide declines may have facilitated the resurgence of
281 hybridization between the nine Delphinoidea species analysed here. If hybridisation did
282 increase, species may already have been sufficiently differentiated that offspring fertility was
283 reduced. Even if offspring were fertile, the high level of differentiation between species may
284 have meant hybrids were unable to occupy either parental niche (Skovrind et al., 2019) and
285 were therefore strongly selected against. A lack of significant contribution from hybrids to
286 the parental gene pools may be why we observe contemporary hybrids, despite lacking
287 evidence of this in the hPSMC analysis.

288 289 **Conclusions**

290
291 Allopatric speciation is generally considered the most common mode of speciation, as
292 the absence of gene flow due to geographical isolation can most easily explain the evolution
293 of ecological, behavioral, morphological, or genetic differences between populations (Norris
294 and Hull, 2012). However, our findings suggest that within Delphinoidea, speciation in the
295 presence of gene flow was commonplace, consistent with sympatric/parapatric speciation.

296
297 Long periods of extended post-divergence gene flow may also explain the presence of
298 contemporaneous hybrids between several species. In parapatric speciation, genetic isolation
299 is achieved relatively early due to geographical and biological isolation, but species develop
300 complete reproductive isolation relatively slowly, allowing hybridization to continue for an
301 extended period of time (Norris and Hull, 2012). The prevalence of this mode of speciation in
302 cetaceans, as suggested by our study and previous genomic analyses (Árnason et al., 2018;
303 Moura et al., 2020), may reflect the low energetic costs of dispersing across large distances in
304 the marine realm (Fish et al., 2008; Williams, 1999) and the relative absence of geographic

305 barriers preventing such dispersal events (Palumbi, 1994). Both factors are believed to be
306 important in facilitating long-distance (including inter-hemispheric and inter-oceanic)
307 movements in many cetacean species (Stone et al., 1990).

308

309 **Methods**

310

311 **Data collection**

312 We downloaded the assembled genomes and raw sequencing reads from nine toothed
313 whales from the superfamily Delphinoidea. The data included five Delphinidae: Indo-Pacific
314 white-sided dolphin (NCBI Biosample: SAMN09386610), Indo-Pacific bottlenose dolphin
315 (NCBI Biosample: SAMN06289676), bottlenose dolphin (NCBI Biosample:
316 SAMN09426418), killer whale (NCBI Biosample: SAMN01180276), and long-finned pilot
317 whale (NCBI Biosample: SAMN11083132); two Phocoenidae: harbour porpoise (available
318 from Autenrieth et al., 2018), finless porpoise (NCBI Biosample: SAMN02192673); and two
319 Monodontidae: beluga (NCBI Biosample: SAMN06216270), narwhal (NCBI Biosample:
320 SAMN10519625). To avoid biases that may occur when mapping to an ingroup reference
321 (Westbury et al., 2019), we used the assembled baiji genome (Genbank accession code:
322 GCF_000442215.1) as mapping reference in the gene flow analyses. Delphinoidea and the
323 baiji diverged ~24.6 Ma (95% CI 25.2 - 23.8 Ma) (McGowen et al., 2020).

324

325 **Initial data filtering**

326 To determine which scaffolds were most likely autosomal in origin, we identified
327 putative sex chromosome scaffolds for each genome, and omitted them from further analysis.
328 We found putative sex chromosome scaffolds in all ten genomes by aligning the assemblies
329 to the Cow X (Genbank accession: CM008168.2) and Human Y (Genbank accession:
330 NC_000024.10) chromosomes. Alignments were performed using satsuma synteny v2.1
331 (Grabherr et al., 2010) with default parameters. We also removed scaffolds smaller than 100
332 kb from all downstream analyses.

333

334 **Mapping**

335 We trimmed adapter sequences from all raw reads using skewer v0.2.2 (Jiang et al.,
336 2014). We mapped the trimmed reads to the baiji for downstream gene flow analyses, and to
337 the species-specific reference genome for downstream demographic history and genetic
338 diversity analyses using BWA v0.7.15 (Li and Durbin, 2009) and the mem algorithm. We
339 parsed the output and removed duplicates and reads with a mapping quality lower than 30
340 with SAMtools v1.6 (Li et al., 2009). Mapping statistics can be found in supplementary tables
341 S3 and S4.

342

343 **Sliding-window phylogeny**

344 For the sliding-window phylogenetic analysis, we created fasta files for all individuals
345 mapped to the baiji genome using a consensus base call (-dofasta 2) approach in ANGSD
346 v0.921 (Korneliussen et al., 2014), and specifying the following filters: minimum read depth
347 of 5 (-mininddepth 5), minimum mapping quality of 30 (-minmapq 30), minimum base
348 quality (-minq 30), only consider reads that map to one location uniquely (-uniqueonly 1),

349 and only include reads where both mates map (-only_proper_pairs 1). All resultant fasta files,
350 together with the assembled baiji genome, were aligned, and sites where any individual had
351 more than 50% missing data were filtered before performing maximum likelihood
352 phylogenetic analyses in a non-overlapping sliding-window approach using RAxML v8.2.10
353 (Stamatakis, 2014). We performed this analysis four times independently, specifying a
354 different window size each time (50 kb, 100 kb, 500 kb, and 1 Mb). We used RAxML with
355 default parameters, specifying baiji as the outgroup, and a GTR+G substitution model. We
356 computed the genome-wide majority rule consensus tree for each window size in PHYLIP
357 (Felsenstein, 2005), with branch support represented by the proportion of trees displaying the
358 same topology. We simultaneously visualised all trees of the same sized window using
359 DensiTree (Bouckaert, 2010).

360

361 **D-statistics**

362 To test for signs of gene flow in the face of incomplete lineage sorting (ILS), we ran
363 D-statistics using all individuals mapped to the baiji genome in ANGSD, using a consensus
364 base call approach (-doabbababa 2), specifying the baiji sequence as the ancestral outgroup
365 sequence, and the same filtering as for the fasta file construction with the addition of setting
366 the block size as 1Mb (-blocksize). Significance of the results was evaluated using a block
367 jackknife approach with the Rscript provided in the ANGSD package. $|Z| > 3$ was deemed
368 significant.

369

370 **D-foil**

371 As D-statistics only tests for the presence and not the direction of gene flow, we ran
372 D-foil (Pease and Hahn, 2015), an extended version of the D-statistics, which is a five-taxon
373 test for gene flow, making use of all four combinations of the potential D-statistics
374 topologies. For this analysis, we used the same fasta files constructed above, which we
375 converted into an mvf file using MVFtools (Pease and Rosenzweig, 2018). We specified the
376 5-taxon [[H1, H2], [H3, H4], baiji], for all possible combinations, following the species tree
377 (Fig. 1) and a 100 kb window size. All scaffolds were trimmed to the nearest 100 kb to avoid
378 the inclusion of windows shorter than 100 kb.

379

380 **Mutation rate estimation**

381 For use in the downstream demographic analyses, we computed the mutation rate per
382 generation for each species. To do this, we estimated the pairwise distances between all
383 ingroup species mapped to the baiji, using a consensus base call in ANGSD (-doIBS 2), and
384 applying the same filters as above, with the addition of only considering sites in which all
385 individuals were covered (-minInd). The pairwise distances used in this calculation were
386 those from the closest lineage to the species of interest (Supplementary tables S5 and S6).
387 The mutation rates per generation were calculated using the resultant pairwise distance as
388 follows: mutation rate = pairwise distance x generation time / 2 x divergence time.
389 Divergence times were taken from the full dataset 10-partition AR (mean) values from
390 McGowen et al. (McGowen et al., 2020) (Supplementary table S6). Generation times were
391 taken from previously published data (Supplementary table S7).

392

393 **Cessation of gene flow**

394 To estimate when gene flow may have ceased between each species pair, we used the
395 F1-hybrid PSMC (hPSMC) approach (Cahill et al., 2016). As input we used the haploid
396 consensus sequences created for the phylogenetic analyses. We merged the haploid sequences
397 from each possible species pair into pseudo-diploid sequences using the scripts available in
398 the hPSMC toolsuite. We independently ran each resultant species pair pseudo-diploid
399 sequences through PSMC, specifying atomic intervals 4+25*2+4+6. We plotted the results
400 using the average (i) mutation rate per generation and (ii) generation time for each species
401 pair being tested. From the output of this analysis, we visually estimated the pre-divergence
402 N_e of each hPSMC plot (i.e. N_e prior to the point of asymptotic increase in N_e) to be used as
403 input for downstream simulations. Based on these empirical results, we ran simulations in ms
404 (Hudson, 2002) using the estimated pre-divergence N_e , and various predefined divergence
405 times to find the interval in which gene flow may have ceased between a given species pair.
406 The time intervals and pre-divergence N_e for each species pair used for the simulations can
407 be seen in supplementary table S8. The ms commands were produced using the scripts
408 available in the hPSMC toolsuite. We plotted the simulated and empirical hPSMC results to
409 find the simulations with an asymptotic increase in N_e closest to, but not overlapping with,
410 the empirical data. The predefined divergence times of the simulations showing this pattern
411 within 1.5x and 10x of the pre-divergence N_e were taken as the time interval in which gene
412 flow ceased.

413

414 **Heterozygosity**

415 As a proxy for species-level genetic diversity, we estimated autosome-wide
416 heterozygosity for each of the nine Delphinoidea species. We estimated autosomal
417 heterozygosity using allele frequencies (-doSaf 1) in ANGSD (Korneliussen et al., 2014),
418 taking genotype likelihoods into account (-GL 2) and specifying the same filters as for the
419 fasta file construction with the addition of adjusting quality scores around indels (-baq 1), and
420 the subsample filter (-downSample), which was uniquely set for each individual to result in a
421 20x genome-wide coverage, to ensure comparability between genomes of differing coverage.
422 Heterozygosity was computed from the output of this using realSFS from the ANGSD
423 toolsuite and specifying 20 Mb windows of covered sites (-nSites).

424

425 **Demographic reconstruction**

426 To determine the demographic histories of all nine species over a two million year
427 time scale, we ran a Pairwise Sequentially Markovian Coalescent model (PSMC) (Li and
428 Durbin, 2011) on each diploid genome independently. We called diploid genome sequences
429 using SAMtools and BCFtools v1.6 (Narasimhan et al., 2016), specifying a minimum quality
430 score of 20 and minimum coverage of 10. We ran PSMC specifying atomic intervals
431 4+25*2+4+6 and performed 100 bootstrap replicates to investigate support for the resultant
432 demographic trajectories. PSMC outputs were plotted using species-specific mutation rates
433 and generation times (Supplementary table S7).

434

435

436

437 **Figure legends:**

438

439 **Figure 1: Sliding-Window Maximum likelihood trees of nine Delphinoidea species and**
440 **the baiji.** Simultaneously plotted trees constructed using non-overlapping sliding windows of
441 (A) 50 kb in length and (B) 1 Mb in length. Black lines show the consensus tree. Grey lines
442 show individual trees. Numbers on branches show the proportion of windows supporting the
443 node. Branches without numbers show 100% support. Baiji, killer whale, white-sided
444 dolphin, pilot whale, harbour porpoise, finless whale, beluga, and narwhal silhouettes: Chris
445 huh, license CC-BY-SA-3.0 (<https://creativecommons.org/licenses/by-sa/3.0/>). Bottlenose
446 dolphin silhouette: license Public Domain Dedication 1.0.

447

448 **Figure 2: Estimated divergence times and time interval during which gene flow ceased**
449 **between species (A) within families and (B) between families.** Estimated time intervals of
450 when gene flow ceased between species pairs are based on hPSMC results and simulated
451 data. Divergence time estimates are taken from the full dataset 10-partition AR results of
452 McGowen et al 2020.

453

454 **Figure 3: Autosome-wide heterozygosity and demographic histories over the last two**
455 **million years.** (A) Autosome-wide levels of heterozygosity calculated in 20 Mb windows of
456 consecutive bases. (B-D) Demographic history of all studied species within (B) Delphinidae,
457 (C) Phocoenidae, and (D) Monodontidae, estimated using PSMC. Thick coloured lines show
458 the autosome-wide demographic history. Faded lines show bootstrap support values.

459

460 **Acknowledgements**

461 The work was supported by the Carlsberg Foundation Distinguished Associate Professor
462 Fellowship, grant no CF16-0202, the Villum Fonden Young Investigator Programme, grant
463 no. 13151, and the Independent Research Fund Denmark | Natural Sciences,
464 Forskningsprojekt 1, grant no. 8021-00218B to EDL. AAC was funded by the Rubicon-NWO
465 grant (project 019.183EN.005). We would like to thank all those contributing to the ever-
466 increasing abundance of publicly available genomic resources. Without the availability of
467 such data, our study would not have been possible.

468

469 **Author contributions**

470 Conceptualization, MVW; Formal analysis, MVW, AAC, AR-I, BDC, SH; Writing –
471 Original Draft MVW; Writing – Review & Editing, All authors; Supervision, MVW, EDL;
472 Funding Acquisition, EDL.

473

474

475

476

477

478

479

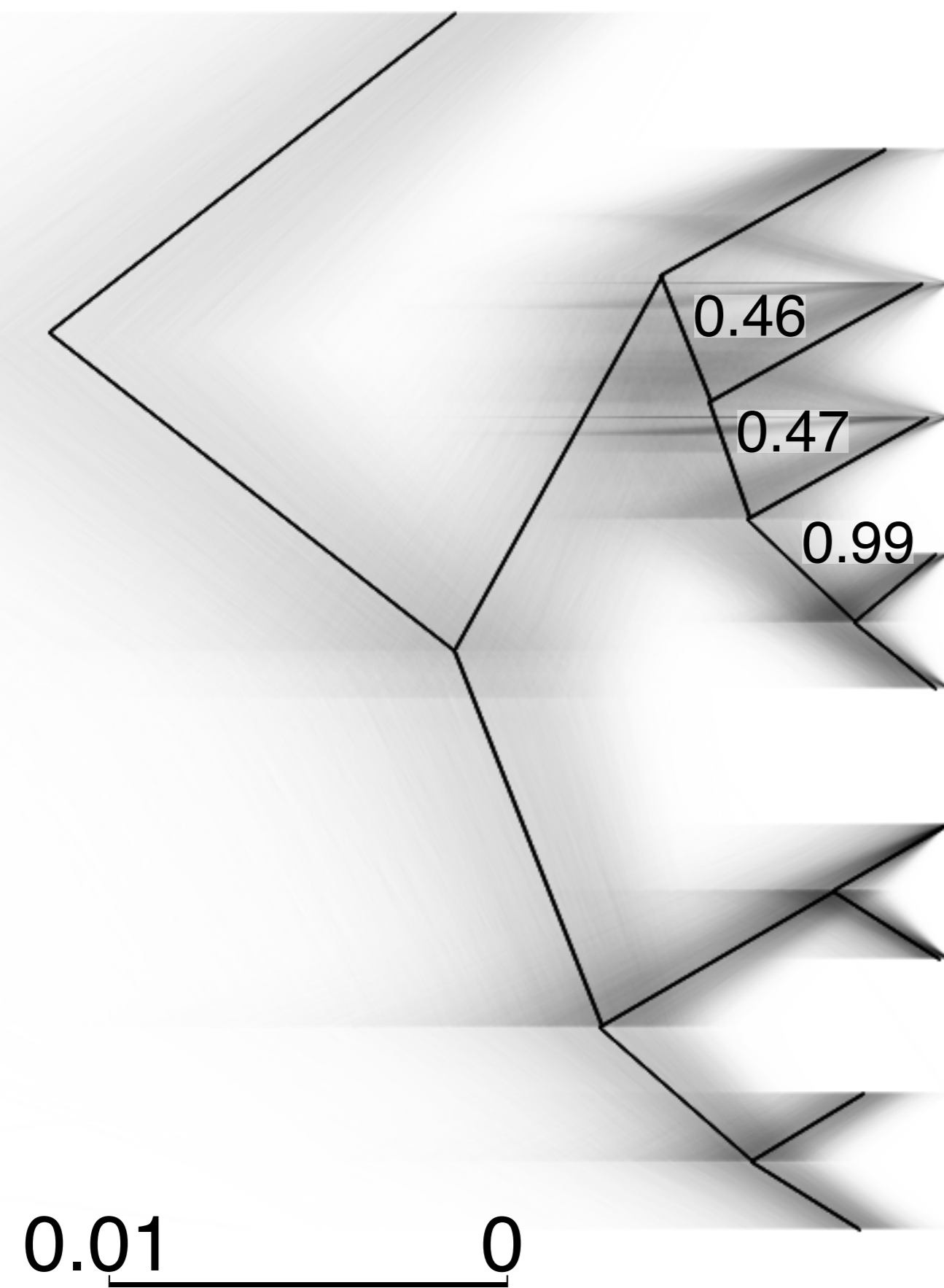
480 **References:**

- 481 Árnason Ú, Lammers F, Kumar V, Nilsson MA, Janke A. 2018. Whole-genome sequencing
482 of the blue whale and other rorquals finds signatures for introgressive gene flow. *Sci Adv*
483 **4**:eaap9873.
- 484 Autenrieth M, Hartmann S, Lah L, Roos A, Dennis AB, Tiedemann R. 2018. High-quality
485 whole-genome sequence of an abundant Holarctic odontocete, the harbour porpoise
486 (*Phocoena phocoena*). *Mol Ecol Resour* **18**:1469–1481.
- 487 Baird RW, Gorgone AM, McSweeney DJ, Ligon AD, Deakos MH, Webster DL, Schorr GS,
488 Martien KK, Salden DR, Mahaffy SD. 2012. Population structure of island-associated
489 dolphins: Evidence from mitochondrial and microsatellite markers for common
490 bottlenose dolphins (*Tursiops truncatus*) in the main Hawaiian Islands. *Mar Mamm Sci*.
491 Barlow A, Cahill JA, Hartmann S, Theunert C, Xenikoudakis G, Fortes GG, Pajmans JLA,
492 Rabeder G, Frischauf C, Grandal-d'Anglade A, García-Vázquez A, Murtskhvaladze M,
493 Saarma U, Anijalg P, Skrbinšek T, Bertorelle G, Gasparian B, Bar-Oz G, Pinhasi R,
494 Slatkin M, Dalén L, Shapiro B, Hofreiter M. 2018. Partial genomic survival of cave
495 bears in living brown bears. *Nat Ecol Evol* **2**:1563–1570.
- 496 Bierne N, Bonhomme F, David P. 2003. Habitat preference and the marine-speciation
497 paradox. *Proc Biol Sci* **270**:1399–1406.
- 498 Bouckaert RR. 2010. DensiTree: making sense of sets of phylogenetic trees. *Bioinformatics*
499 **26**:1372–1373.
- 500 Butlin RK, Smadja CM. 2018. Coupling, Reinforcement, and Speciation. *Am Nat* **191**:155–
501 172.
- 502 Cabrera AA, Schall E, Bérubé M, Bachmann L, Berrow S, Best PB, Clapham PJ, Cunha HA,
503 Rosa LD, Dias C, Findlay KP, Haug T, Heide-Jørgensen MP, Kovacs KM, Landry S,
504 Larsen F, Lopes XM, Lydersen C, Mattila DK, Oosting T, Pace RM, Papetti C, Paspati
505 A, Pastene LA, Prieto R, Ramp C, Robbins J, Ryan C, Sears R, Secchi ER, Silva MA,
506 Víkingsson G, Wiig Ø, Øien N, Palsbøll PJ. 2018. Strong and lasting impacts of past
507 global warming on baleen whale and prey abundance. *bioRxiv*.
- 508 Cahill JA, Soares AER, Green RE, Shapiro B. 2016. Inferring species divergence times using
509 pairwise sequential Markovian coalescent modelling and low-coverage genomic data.
510 *Philos Trans R Soc Lond B Biol Sci* **371**. doi:10.1098/rstb.2015.0138
- 511 Campbell CR, Poelstra JW. 2018. What is Speciation Genomics? The roles of ecology, gene
512 flow, and genomic architecture in the formation of species. *Biol J Linn Soc Lond*
513 **124**:561–583.
- 514 Coyne JA, Orr HA. 2004. Speciation. Sinauer Associates Sunderland, MA.
- 515 Crossman CA, Taylor EB, Barrett-Lennard LG. 2016. Hybridization in the Cetacea:
516 widespread occurrence and associated morphological, behavioral, and ecological factors.
517 *Ecol Evol* **6**:1293–1303.
- 518 Edwards CJ, Suchard MA, Lemey P, Welch JJ, Barnes I, Fulton TL, Barnett R, O'Connell
519 TC, Coxon P, Monaghan N, Valdiosera CE, Lorenzen ED, Willerslev E, Baryshnikov
520 GF, Rambaut A, Thomas MG, Bradley DG, Shapiro B. 2011. Ancient hybridization and
521 an Irish origin for the modern polar bear matriline. *Curr Biol* **21**:1251–1258.
- 522 Espada R, Olaya-Ponzzone L, Haasova L, Martín E, García-Gómez JC. 2019. Hybridization in
523 the wild between *Tursiops truncatus* (Montagu 1821) and *Delphinus delphis* (Linnaeus
524 1758). *PLoS One* **14**:e0215020.
- 525 Feder JL, Egan SP, Nosil P. 2012. The genomics of speciation-with-gene-flow. *Trends Genet*
526 **28**:342–350.
- 527 Felsenstein J. 2005. PHYLIP (Phylogeny Inference Package) version 3.6.
- 528 Fish FE, Howle LE, Murray MM. 2008. Hydrodynamic flow control in marine mammals.

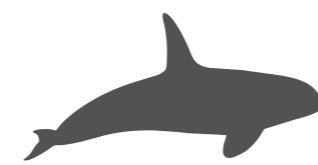
- 529 *Integr Comp Biol* **48**:788–800.
- 530 Foote AD, Morin PA. 2015. Sympatric speciation in killer whales? *Heredity* **114**:537–538.
- 531 Foote AD, Morin PA, Durban JW, Willerslev E. 2011. Out of the Pacific and back again:
532 insights into the matrilineal history of Pacific killer whale ecotypes. *PLoS*.
- 533 Grabherr MG, Russell P, Meyer M, Mauceli E, Alföldi J, Di Palma F, Lindblad-Toh K. 2010.
534 Genome-wide synteny through highly sensitive sequence alignment: Satsuma.
535 *Bioinformatics* **26**:1145–1151.
- 536 Gridley T, Elwen SH, Harris G, Moore DM, Hoelzel AR, Lampen F. 2018. Hybridization in
537 bottlenose dolphins—A case study of *Tursiops aduncus* × *T. truncatus* hybrids and
538 successful backcross hybridization events. *PLoS One* **13**:e0201722.
- 539 Herzing DL, Johnsonz CM. 1997. Interspecific interactions between Atlantic spotted
540 dolphins (*Stenella frontalis*) and bottlenose dolphins (*Tursiops truncatus*) in the
541 Bahamas 1985-1995. *Aquat Mamm*.
- 542 Hudson RR. 2002. Generating samples under a Wright–Fisher neutral model of genetic
543 variation. *Bioinformatics* **18**:337–338.
- 544 Jiang H, Lei R, Ding S-W, Zhu S. 2014. Skewer: a fast and accurate adapter trimmer for
545 next-generation sequencing paired-end reads. *BMC Bioinformatics* **15**:182.
- 546 Korneliussen TS, Albrechtsen A, Nielsen R. 2014. ANGSD: Analysis of Next Generation
547 Sequencing Data. *BMC Bioinformatics* **15**:356.
- 548 Leaché AD, Harris RB, Rannala B, Yang Z. 2014. The influence of gene flow on species tree
549 estimation: a simulation study. *Syst Biol* **63**:17–30.
- 550 Li H, Durbin R. 2011. Inference of human population history from individual whole-genome
551 sequences. *Nature* **475**:493–496.
- 552 Li H, Durbin R. 2009. Fast and accurate short read alignment with Burrows–Wheeler
553 transform. *Bioinformatics* **25**:1754–1760.
- 554 Li H, Handsaker B, Wysoker A, Fennell T, Ruan J, Homer N, Marth G, Abecasis G, Durbin
555 R, 1000 Genome Project Data Processing Subgroup. 2009. The Sequence
556 Alignment/Map format and SAMtools. *Bioinformatics* **25**:2078–2079.
- 557 Liu S, Lorenzen ED, Fumagalli M, Li B, Harris K, Xiong Z, Zhou L, Korneliussen TS, Somel
558 M, Babbitt C, Wray G, Li J, He W, Wang Z, Fu W, Xiang X, Morgan CC, Doherty A,
559 O’Connell MJ, McInerney JO, Born EW, Dalén L, Dietz R, Orlando L, Sonne C, Zhang
560 G, Nielsen R, Willerslev E, Wang J. 2014. Population genomics reveal recent speciation
561 and rapid evolutionary adaptation in polar bears. *Cell* **157**:785–794.
- 562 McGowen MR, Tsagkogeorga G, Álvarez-Carretero S, Dos Reis M, Struebig M, Deaville R,
563 Jepson PD, Jarman S, Polanowski A, Morin PA, Rossiter SJ. 2020. Phylogenomic
564 Resolution of the Cetacean Tree of Life Using Target Sequence Capture. *Syst Biol*
565 **69**:479–501.
- 566 Miralles L, Oremus M, Silva MA, Planes S, Garcia-Vazquez E. 2016. Interspecific
567 Hybridization in Pilot Whales and Asymmetric Genetic Introgression in Northern
568 Globicephala melas under the Scenario of Global Warming. *PLoS One* **11**:e0160080.
- 569 Miyazaki N, Hirotsuki Y, Kinuta T, Omura H. 1992. Osteological study of a hybrid between
570 *Tursiops truncatus* and *Grampus griseus*. *Bull Natl Mus Nat Sci Ser B Bot* **18**:79–94.
- 571 Moodley Y, Westbury MV, Russo I-RM, Gopalakrishnan S, Rakotoarivelo A, Olsen R-A,
572 Prost S, Tunstall T, Ryder OA, Dalén L, Bruford MW. 2020. Interspecific gene flow and
573 the evolution of specialisation in black and white rhinoceros. *Mol Biol Evol*.
574 doi:10.1093/molbev/msaa148
- 575 Moura AE, Kenny JG, Chaudhuri RR, Hughes MA. 2015. Phylogenomics of the killer whale
576 indicates ecotype divergence in sympatry. *Heredity* **114**:48–55.
- 577 Moura AE, Shreves K, Pilot M, Andrews KR, Moore DM, Kishida T, Möller L, Natoli A,
578 Gaspari S, McGowen M, Chen I, Gray H, Gore M, Culloch RM, Kiani MS, Willson MS,

- 579 Bulushi A, Collins T, Baldwin R, Willson A, Minton G, Ponnampalam L, Hoelzel AR.
580 2020. Phylogenomics of the genus *Tursiops* and closely related Delphininae reveals
581 extensive reticulation among lineages and provides inference about eco-evolutionary
582 drivers. *Mol Phylogenet Evol* **146**:106756.
- 583 Narasimhan V, Danecek P, Scally A, Xue Y, Tyler-Smith C, Durbin R. 2016. BCFtools/RoH:
584 a hidden Markov model approach for detecting autozygosity from next-generation
585 sequencing data. *Bioinformatics* **32**:1749–1751.
- 586 Norris RD, Hull PM. 2012. The temporal dimension of marine speciation. *Evol Ecol* **26**:393–
587 415.
- 588 Palumbi SR. 1994. Genetic divergence, reproductive isolation, and marine speciation. *Annu*
589 *Rev Ecol Syst* **25**:547–572.
- 590 Pease JB, Hahn MW. 2015. Detection and Polarization of Introgression in a Five-Taxon
591 Phylogeny. *Syst Biol* **64**:651–662.
- 592 Pease JB, Rosenzweig BK. 2018. Encoding Data Using Biological Principles: The
593 Multisample Variant Format for Phylogenomics and Population Genomics. *IEEE/ACM*
594 *Trans Comput Biol Bioinform* **15**:1231–1238.
- 595 Polyak VJ, Onac BP, Fornós JJ, Hay C, Asmerom Y, Dorale JA, Ginés J, Tuccimei P, Ginés
596 A. 2018. A highly resolved record of relative sea level in the western Mediterranean Sea
597 during the last interglacial period. *Nat Geosci* **11**:860–864.
- 598 Silva JM, Silva FJL, Sazima I. 2005. Two presumed interspecific hybrids in the genus
599 *Stenella* (Delphinidae) in the Tropical West Atlantic. *Aquat Mamm* **31**:468.
- 600 Skovrind M, Castruita JAS, Haile J, Treadaway EC, Gopalakrishnan S, Westbury MV,
601 Heide-Jørgensen MP, Szpak P, Lorenzen ED. 2019. Hybridization between two high
602 Arctic cetaceans confirmed by genomic analysis. *Sci Rep* **9**:7729.
- 603 Slatkin M, Pollack JL. 2008. Subdivision in an ancestral species creates asymmetry in gene
604 trees. *Mol Biol Evol* **25**:2241–2246.
- 605 Stamatakis A. 2014. RAxML version 8: a tool for phylogenetic analysis and post-analysis of
606 large phylogenies. *Bioinformatics* **30**:1312–1313.
- 607 Steeman ME, Hebsgaard MB, Fordyce RE, Ho SYW, Rabosky DL, Nielsen R, Rahbek C,
608 Glenner H, Sørensen MV, Willerslev E. 2009. Radiation of extant cetaceans driven by
609 restructuring of the oceans. *Syst Biol* **58**:573–585.
- 610 Stone G, Florez-Gonzalez L, Katona S. 1990. Whale migration record. *Nature* **346**:705–705.
- 611 Turelli M, Barton NH, Coyne JA. 2001. Theory and speciation. *Trends Ecol Evol* **16**:330–
612 343.
- 613 Westbury MV, Hartmann S, Barlow A, Preick M, Ridush B, Nagel D, Rathgeber T, Ziegler
614 R, Baryshnikov G, Sheng G, Ludwig A, Wiesel I, Dalen L, Bibi F, Werdelin L, Heller
615 R, Hofreiter M. 2020. Hyena paleogenomes reveal a complex evolutionary history of
616 cross-continental gene flow between spotted and cave hyena. *Science Advances*
617 **6**:eaay0456.
- 618 Westbury MV, Petersen B, Lorenzen ED. 2019. Genomic analyses reveal an absence of
619 contemporary introgressive admixture between fin whales and blue whales, despite
620 known hybrids. *PLoS One* **14**:e0222004.
- 621 Williams TM. 1999. The evolution of cost efficient swimming in marine mammals: limits to
622 energetic optimization. *Philosophical Transactions of the Royal Society of London*
623 *Series B: Biological Sciences* **354**:193–201.
- 624 Willis PM, Crespi BJ, Dill LM, Baird RW, Hanson MB. 2004. Natural hybridization between
625 Dall's porpoises (*Phocoenoides dalli*) and harbour porpoises (*Phocoena phocoena*). *Can*
626 *J Zool* **82**:828–834.
- 627 Zheng Y, Janke A. 2018. Gene flow analysis method, the D-statistic, is robust in a wide
628 parameter space. *BMC Bioinformatics* **19**:10.

A



Baiji



Killer whale



White-sided dolphin



Pilot whale



Bottlenose dolphin



Indo bottlenose dolphin



Harbour porpoise



Finless porpoise

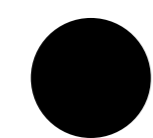
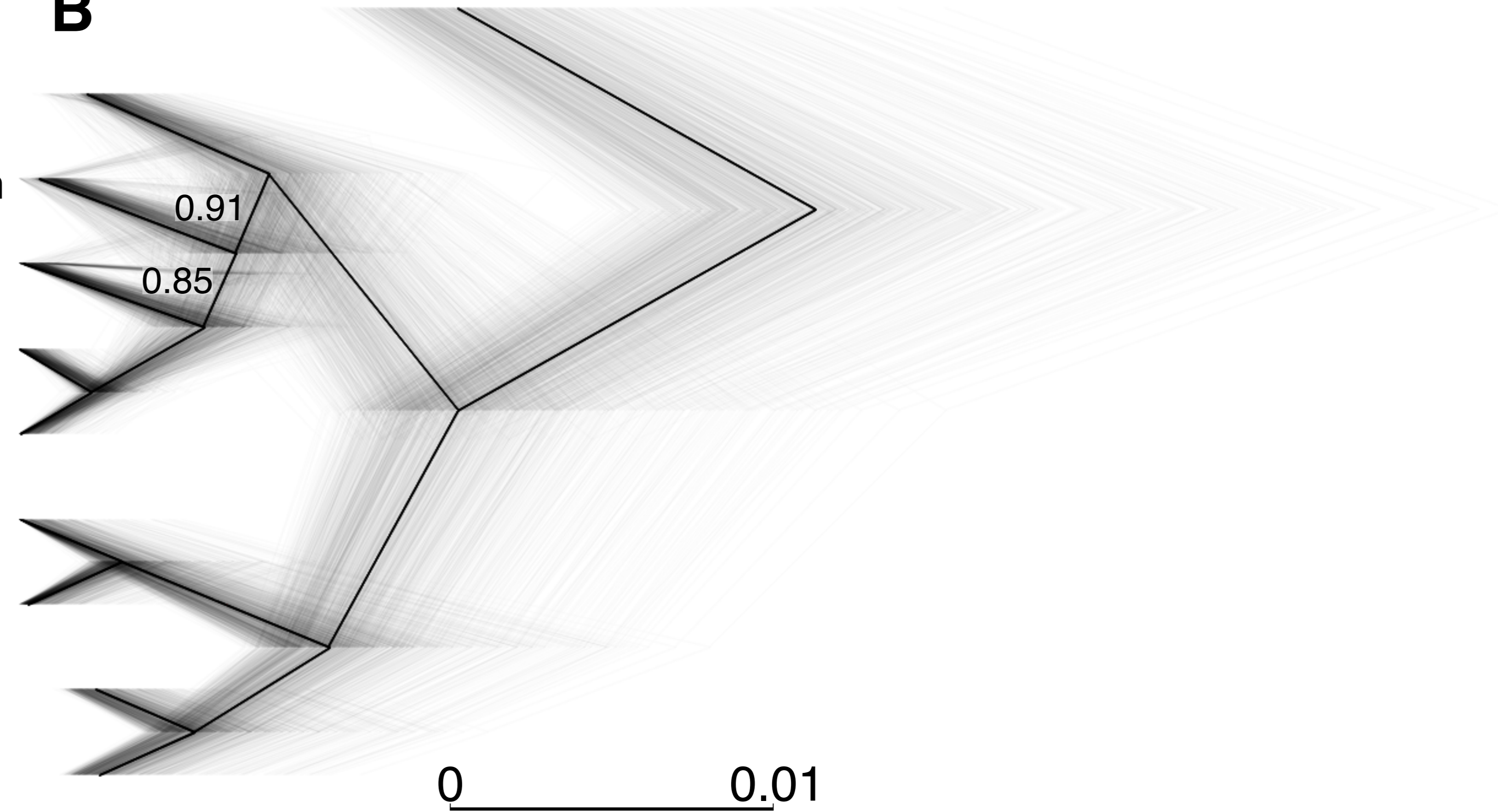


Beluga



Narwhal

B



Outgroup



Delphinidae

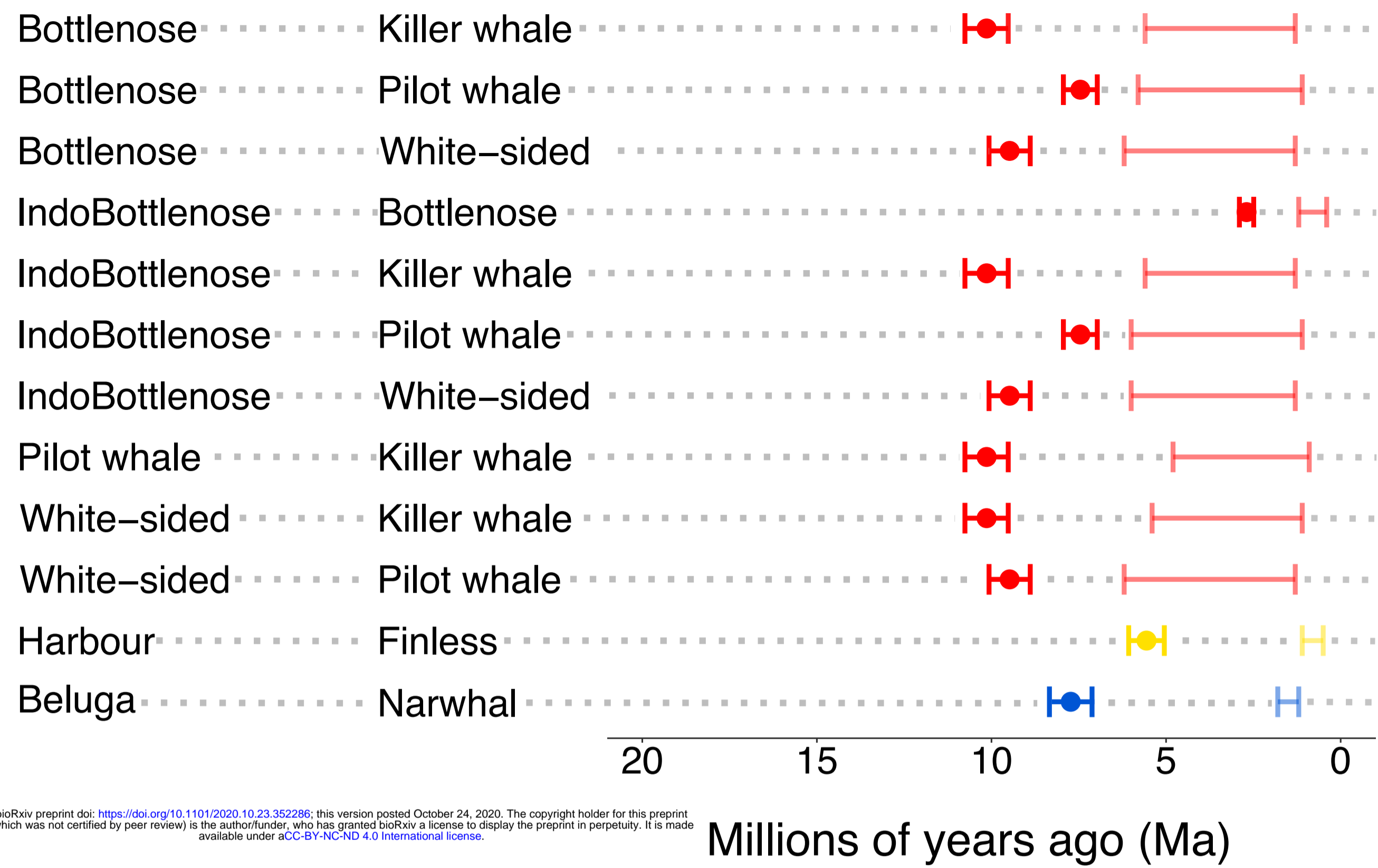


Phocoenidae

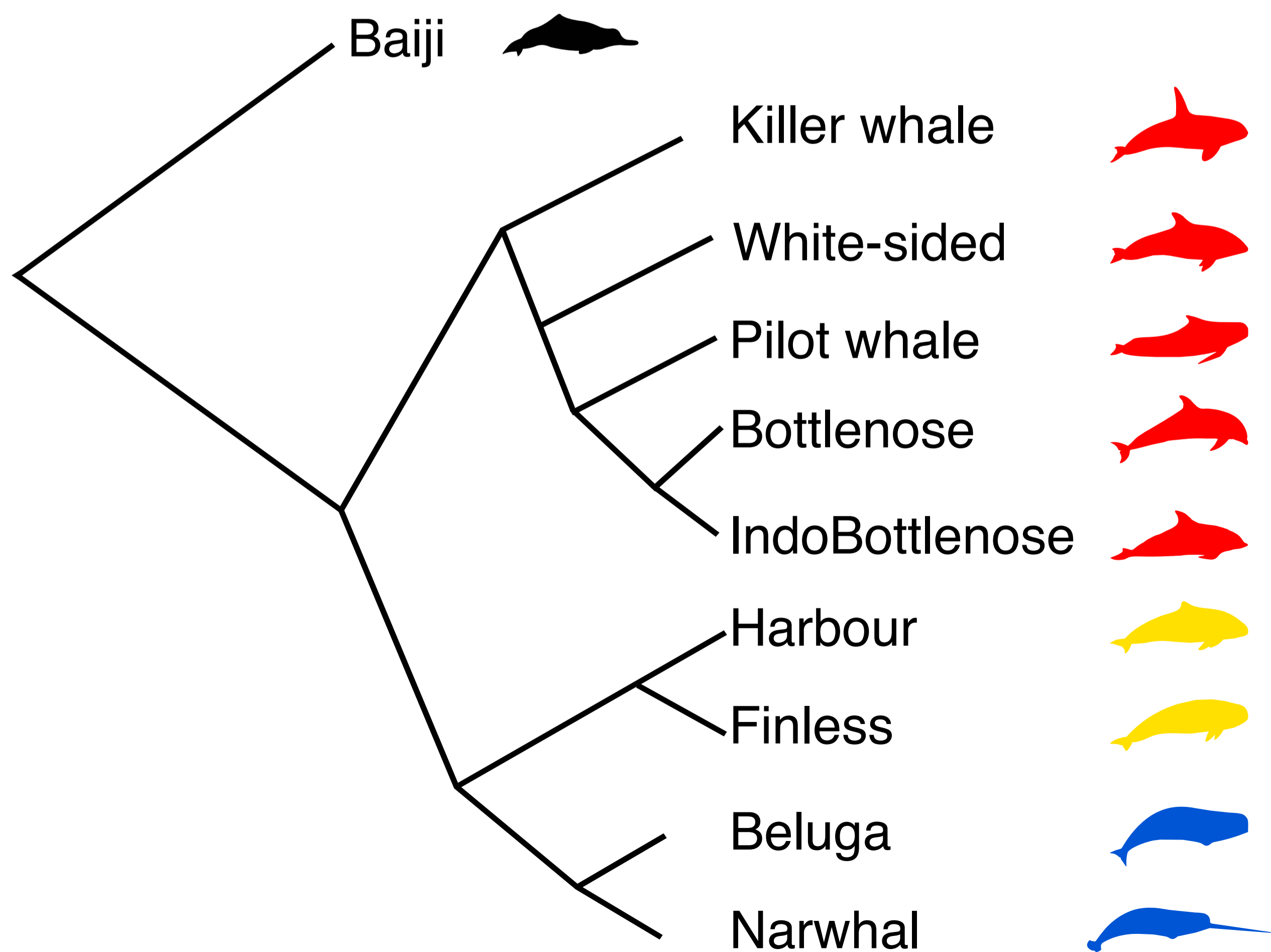


Monodontidae

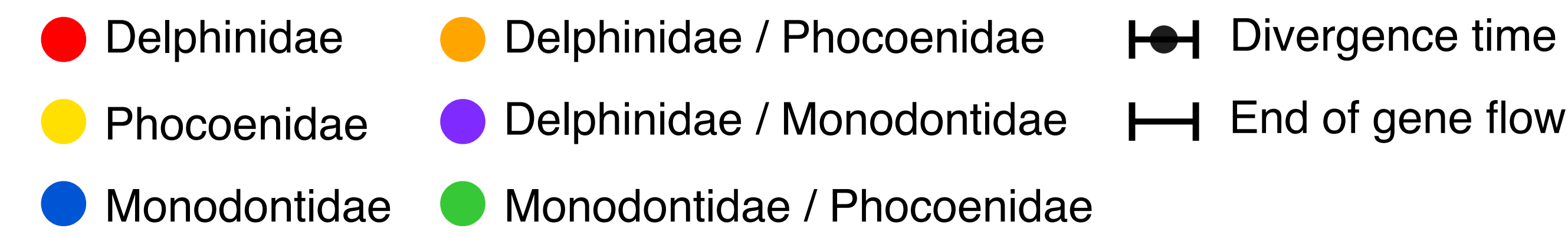
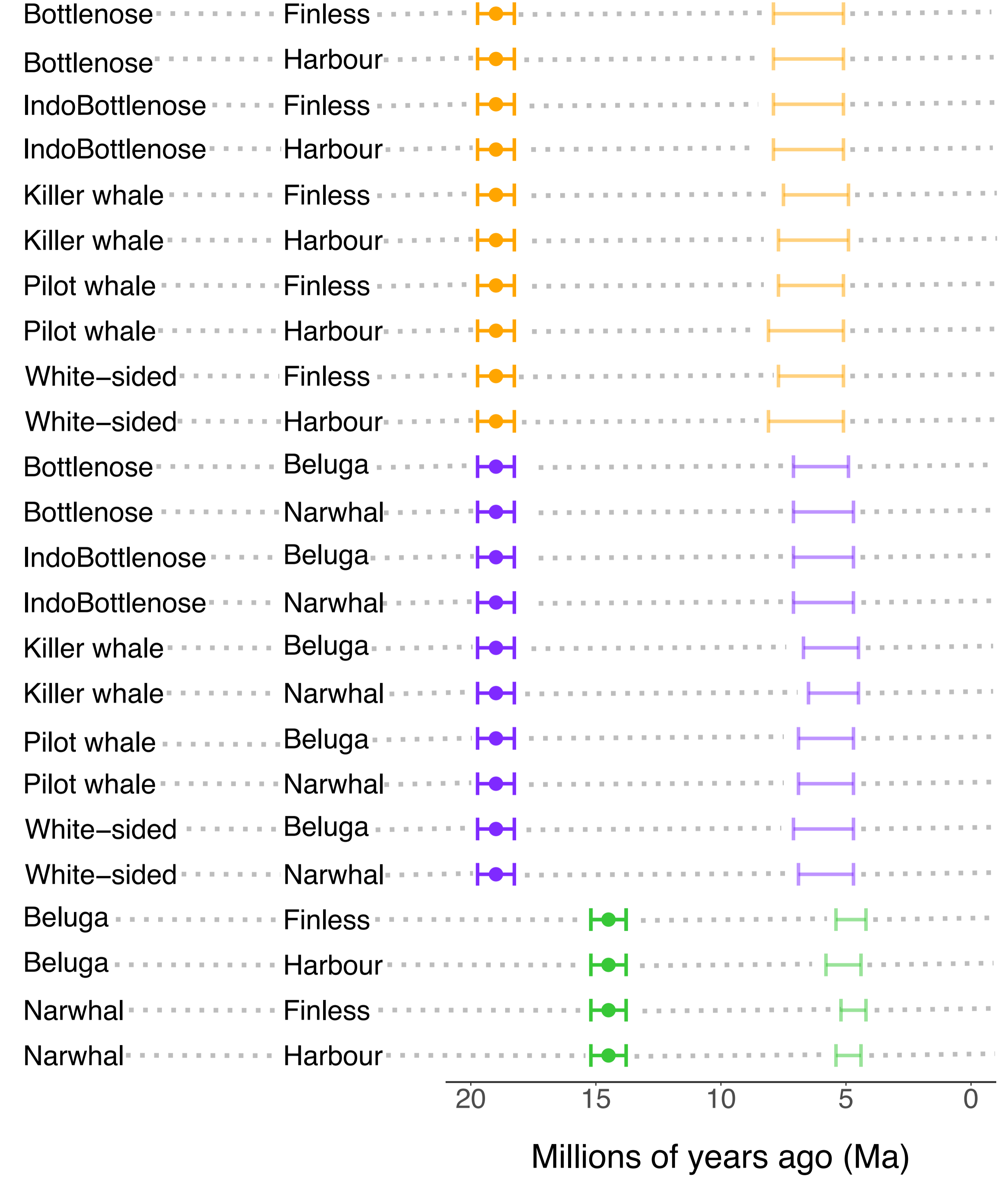
A Within families

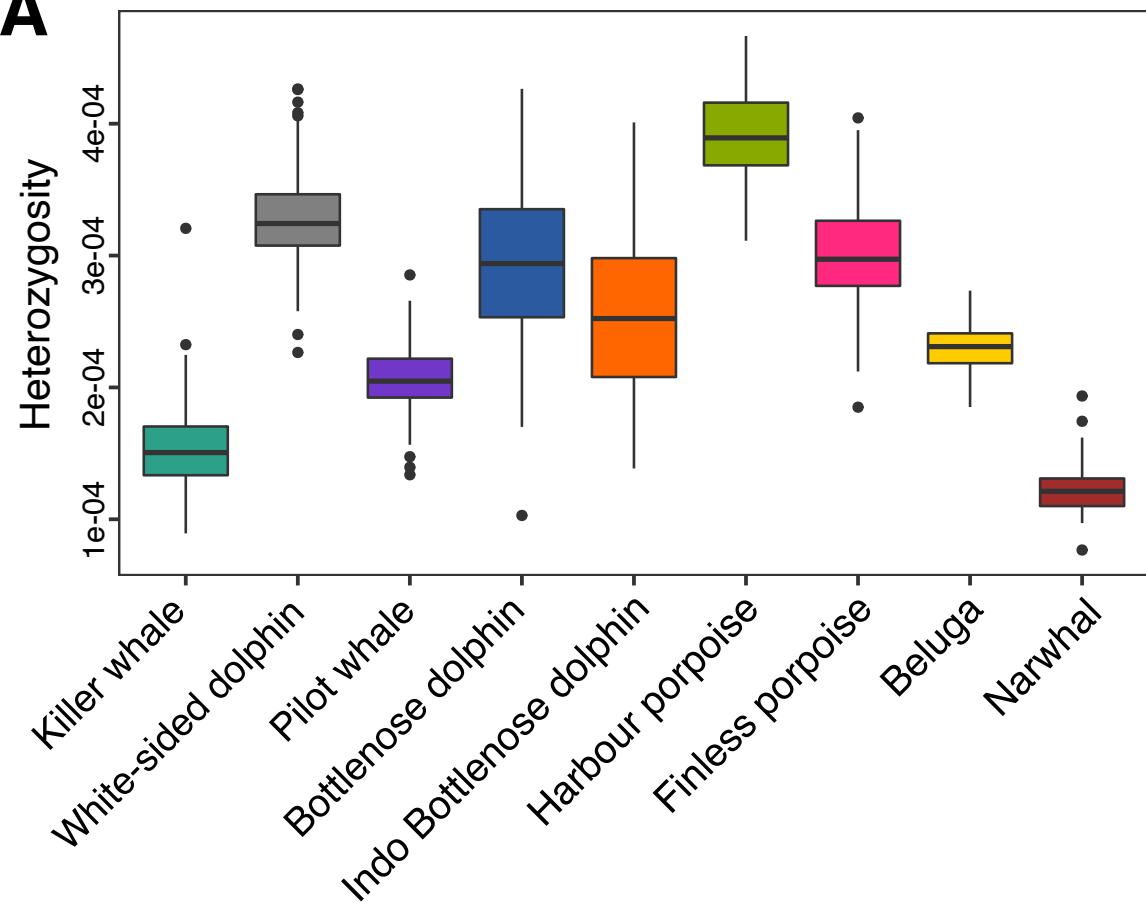


bioRxiv preprint doi: <https://doi.org/10.1101/2020.10.23.352286>; this version posted October 24, 2020. The copyright holder for this preprint (which was not certified by peer review) is the author/funder, who has granted bioRxiv a license to display the preprint in perpetuity. It is made available under aCC-BY-NC-ND 4.0 International license.





B Between families



A**Delphinidae**

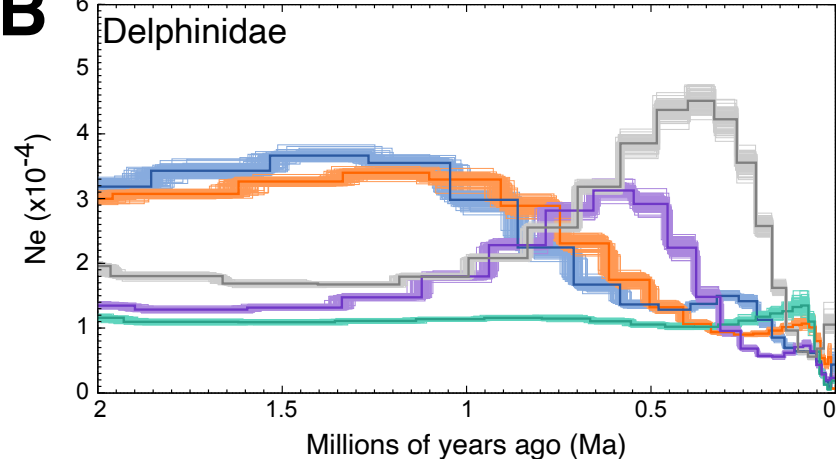
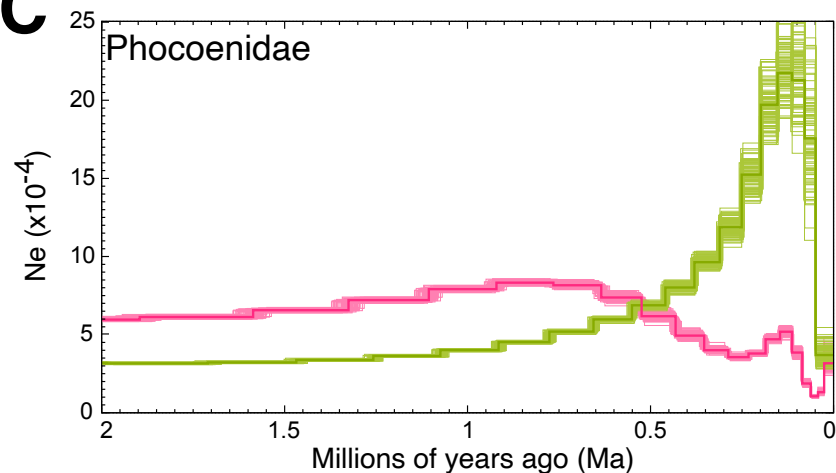
-  Killer whale
-  White-sided dolphin
-  Pilot whale
-  Bottlenose dolphin
-  Indo bottlenose dolphin

Phocoenidae

-  Harbour porpoise
-  Finless porpoise

Monodontidae

-  Beluga
-  Narwhal

B**C****D**